JOURNAL OF CATALYSIS 130, 21–28 (1991)

EXAFS Characterization of the Adsorbed State of Ni(II) Ions in Ni/SiO_2 Materials Prepared by Deposition–Precipitation

O. CLAUSE,[1,*] L. BONNEVIOT,* M. CHE,* AND H. DEXPERT†

*Laboratoire de Réactivité de Surface et Structure, URA 1106 CNRS, Université Pierre et Marie Curie, 4 place Jussieu, 75252-Paris Cedex 05; and †LURE, Université Paris-Sud, 91405 Orsay, France

Received August 13, 1990; revised January 3, 1991

Ni/SiO_2 materials have been prepared by the deposition–precipitation technique. After washing and drying, the unreduced and uncalcined materials have been investigated by EXAFS spectroscopy, temperature-programmed reduction (TPR), and electron microscopy. The formation of nickel silicates likely of nepouite structure, $Ni_3Si_2O_5(OH)_4$, is established by EXAFS and confirmed by TPR experiments in contrast to X-ray diffraction which does not provide any information. The obtainment of high nickel content involves a partial dissolution of silica followed by a reprecipitation leading to the silicate formation. While EXAFS indicates the formation of silicates and excludes the precipitation of $Ni(OH)_2$ epitaxially "glued" onto silicate layers, TPR excludes the precipitation of $Ni(OH)_2$ in the pores of the washed materials.

INTRODUCTION

The oxide supports used as carriers to disperse metal particles are often versatile entities that play numerous roles (*1, 2*) : they can act as microporous containers (*3, 4*), macroanions (*5, 6*), ligands (*7–9*), or as a chemical reagent (*1, 10*). This versatile behavior emphasizes the importance of the catalysts preparation. Incipient wetness impregnation often leads to weak active phase-support interactions and hence to poor oxide particle dispersions, although more complex interactions between the ions and the carrier may occur simultaneously (*11*). The ion-exchange method frequently leads to high and homogeneous dispersions but also to low metallic contents. Deposition–precipitation of metal precursors on supports when accompanied by adsorption is recognized to give high and homogeneous dispersions even at high metallic contents (*12*). In the case of Ni/SiO_2 catalysts, a strong interaction between Ni(II) ions and silica occurs which has been clearly evidenced by typical pH curves as a function of preparation time (*10*). The present paper reports on results on Ni/SiO_2 materials prepared by deposition–precipitation, which has been the subject of recent papers (*13–15*) and on the nature of this strong interaction by means of EXAFS characterization. A following paper will discuss the behavior of these catalysts under calcination or reducing treatments in comparison with Ni/SiO_2 prepared by incipient wetness impregnation or ion-exchange method.

EXPERIMENTAL

Materials Preparation

Ni/SiO_2 materials have been prepared by a controlled-pH urea deposition technique developed by Van Dillen and co-workers (*17*). A slow and homogeneous increase of OH^- concentration is required to obtain deposition–precipitation. The hydrolysis of urea at 90°C is used as the source of hydroxide ions. A suspension of 6 g of SPHEROSIL XOA 400 silica (provided by Rhône-Poulenc; specific surface area 400 m^2/g;

[1] To whom correspondence should be addressed at Institut Français du Petrole, BP311, 92 506 Rueil-Malmaison, France.

0021-9517/91 $3.00

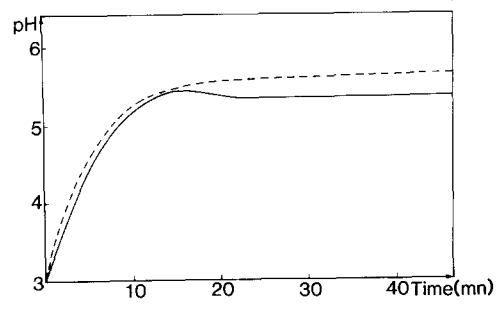

FIG. 1. pH of the nickel nitrate solution as a function of the urea decomposition time at 363 K. Dotted line: without silica. Solid line: with silica (deposition–precipitation).

mean pore diameter 8 nm) in 100 cc of a 0.25 *M* nickel nitrate (PROLABO) and 0.87 *M* urea (JANSSEN) solution is agitated and heated until a temperature of 90°C is reached. The suspension is stirred at this temperature for 20 min (sample A), 1 h (sample B), 3 h (sample C), and 72 h (sample D). The silica gel is filtered, washed on a Büchner until washing solutions become transparent, and finally dried overnight at 100°C. Nickel contents are determined by chemical analysis using atomic absorption after acid extraction, see Table 1. The temperature and the pH of the solutions were recorded during deposition–precipitation as a function of time with a TACUSSEL pH meter. The influence of the silica suspension on the pH measurements was found to be negligible. The pH time dependence during urea hydrolysis is presented in Fig. 1 (full line). The final pH is 5.4. The pH curve in absence of silica (nickel hydroxide precipitation) is also plotted. The pH curves are very similar to those reported by Burch and Flambard (*15*) and are characteristic of the deposition–precipitation operation.

EXAFS Characterization

EXAFS measurements were performed at the LURE radiation synchrotron facility using the X-ray beam emitted by the DCI storage ring. The energy was scanned with 2-eV steps starting from 100 eV below the K absorption edge of Ni (8331 eV), using a channel-cut single crystal of silicon as monochromator. Amplitude and phase functions for O, Ni, and Si neighbors were obtained experimentally for the spectra of NiO (six O neighbors at 2.09 Å), well crystallized $Ni(OH)_2$ (six Ni neighbors at 3.14 Å), and a Ni-doped magnesium hydroxide Ni: Mg $(OH)_2$ (6 Mg at 3.14 Å). The latter compound may be considered a convenient reference for Si neighbors since the masses of Si and Mg are very close. The number of neighbors, distances, and Debye–Waller factors of the reference compounds are gathered in Table 2.

The analysis of the EXAFS spectra was performed following standard procedure for background removal and normalization to the edge absorption. Two synthetic silicates, Ni-talc of formula $Ni_3Si_4O_{10}(OH)_2$ and a Ni-nepouite of formula $Ni_3Si_2O_5(OH)_4$ used as complementary references for the Debye–Waller factors calibration were kindly supplied by A. Decarreau.

Temperature-Programmed Reduction

The samples (between 25 and 100 mg of Ni/SiO_2 materials) are placed into a quartz bed reactor and reduced by a flow of 5% hydrogen in argon (Air Liquide). The reactor is placed in a tubular furnace. The temperature is increased linearly at a rate of 7.5°C/min from 25 to 900°C. The loss of hydrogen from the reducing stream is detected by a catharometer and is proportional to the rate of reduction of the sample at a given time (or temperature). The TPR profiles were normalized with respect to the amount of nickel present.

TABLE 1

Sample Preparation

Sample	A	B	C	D
Deposition–precipitation time (h)	0.3	1	3	72
Nickel content (wt%)	1.5	2.5	7.5	17.5

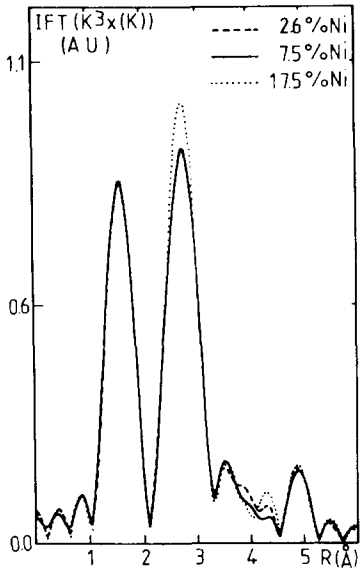

FIG. 2. EXAFS spectra after k^3-weighted Fourier transform of samples B, C, and D without phase corrections.

Transmission Electron Microscopy (TEM)

The transmission electron microscopy studies were performed on a JEM 120 CX JEOL apparatus.

X-ray Diffraction

Powder X-ray diffraction analysis was carried out with a Enraf–Nonius diffractometer using Ni-filtered Cu$K\alpha$ radiation.

RESULTS

Nickel Contents

The nickel contents of Ni/SiO_2 materials after washing and drying overnight at 100°C are listed in Table 1.

EXAFS Characterization

The EXAFS spectra of the samples B, C, and D after k^3-weighted Fourier transform are shown in Fig. 2. We could not perform any EXAFS measurement with sample A: its too weak nickel content (1.5 wt%) did not allow any accurate EXAFS analysis in transmission mode to be made. The nearest peak from the origin of each spectrum corresponds to oxygen neighbors (first or nearest neighbors). For all samples, the number of O neighbors, the distances Ni–O, and the Debye–Waller factors calculated from reference spectra (Table 2) are 5.9 neighbors, 2.04 Å, and 0.09 Å, respectively. The number of oxygen neighbors, close to six, characterizes Ni(II) in an octahedral environment: the local symmetry around Ni(II) ions is not modified by the deposition–precipitation. The next nearest peaks correspond to the second coordination shells. As the spectra of samples B, C, and D are very similar, the calculated compositions of the second peaks are obviously identical. The analysis of the second peaks shows that silicon and nickel ions are

TABLE 2

Structural Parameters of the Reference Compounds

Reference compound	Shell atom	Distance (Å) (XRD)	Number	σ (Å)	Q	Reference
NiO	O	2.09	6	0.11	—	(*18*)
$Ni(OH)_2$	Ni	3.12	6	0.09	—	(*18*)
$Ni:Mg(OH)_2$	Mg	3.14	6	0.09	—	(*18*)
Ni-nepouite	Ni	3.08	6.0	0.09	0.0016	This work
	Si	3.27	2.4	0.07		
Ni-talc	Ni	3.05	6.0	0.09	0.0044	This work
	Si	3.27	4.9	0.06		

Note. The best fits for the Ni-neopouite and the Ni-talc are obtained by minimizing the agreement factor Q. $\Gamma = 1.0$ Å^{-2} for all samples.

TABLE 3

Structural Parameters of the Ni/SiO_2 Samples Determined by EXAFS Spectroscopy

Sample		Ni			Si			Q
		N	R(Å)	σ(Å)	N	R(Å)	σ(Å)	
B	1st fit	5.9	3.10	0.10	2.4	3.37	0.07	0.0049
	2d fit	4.1	3.10	0.08	4.0	3.31	0.08	0.0052
C	1st fit	5.8	3.10	0.10	2.4	3.37	0.07	0.0048
	2d fit	4.0	3.10	0.08	4.0	3.31	0.08	0.0056
D	1st fit	6.0	3.09	0.09	3.1	3.36	0.07	0.0044
	2d fit	4.3	3.10	0.08	4.1	3.31	0.08	0.0020

present in the second shell of coordination (Table 3). Nevertheless, the mathematical fitting of the second peaks does not give a unique solution: four Ni and four Si neighbors in the second shell of coordination are as acceptable as six Ni and two Si neighbors. Two sets of fits, the first one corresponding to six Ni and two Si retrodiffusors and the second one corresponding to four Ni and four Si retrodiffusors are given in Table 3. We observe that the agreement factors quantifying the differences between the fits and the experimental data are of the same order of magnitude for both sets of fits. The correct solutions are thus mathematically undistinguishable. The physical meaning of both sets of fits is however very different: the first fits characterize silicate platelets of nepouite-like structure ($Ni_3Si_2O_5(OH)_4$), whose sizes are larger than 50 Å (*18*). The second fits characterize silicate platelets of talc-like structure ($Ni_3Si_4O_{10}(OH)_2$) smaller than 30 Å. The correct solutions have been selected as follows: the second peaks for a synthetic Ni-talc and a synthetic Ni-nepouite characterized by their XRD pattern were fitted knowing that the exact composition was in the case of the Ni-talc, six Ni and four Si neighbors and, in the case of the nepouite, six Ni and two Si neighbors (Table 2). The Debye–Waller factors characterize the disorder in the structure: their values for synthetized silicates, indicated in Table 2, $\sigma_{Ni} = 0.09$ and $\sigma_{Si} = 0.07$, may be considered as the minimal values convenient for the corresponding retrodiffusors in the fits of samples B, C, and D, the silicates present in these samples being X-ray amorphous and thus very badly crystallized: therefore the fits with four Ni and four Si neighbors are not acceptable with respect to the Debye–Waller factor σ_{Ni}, inferior to the corresponding factor in the synthetized silicates. Correct values of N_{Ni} and N_{Si} are close to 6 and 2 respectively for the Ni/SiO_2 samples independent of the nickel contents. This result is consistent with the presence of Ni-nepouite-like silicate platelets whose sizes are likely larger than 50 Å.

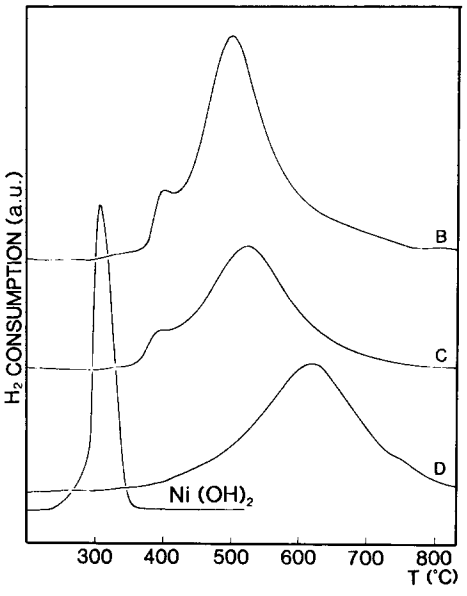

FIG. 3. Temperature-programmed reduction profiles of Ni/SiO_2 materials prepared by deposition–precipitation with 2.5% (sample B), 7.5% (sample C), 17.5% (sample D) Ni wt% without prior calcination, and of the $Ni(OH)_2$ reference.

FIG. 4. Electron micrographs of Ni/SiO_2 materials prepared by deposition–precipitation with (a) 7.5% (sample C), (b) 17.5% (sample D) Ni wt% without prior calcination (magnification by a factor of 230,000).

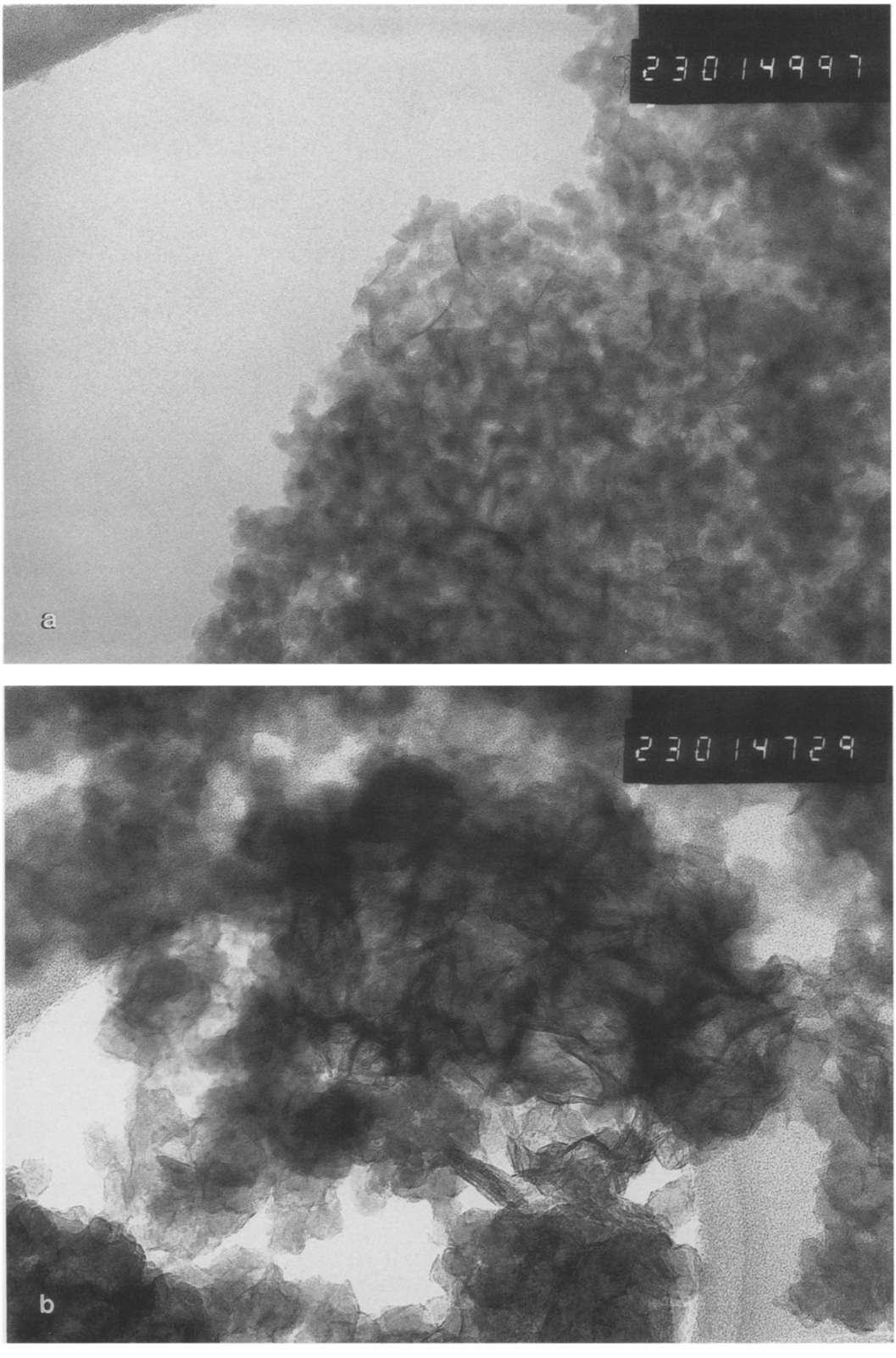
23014997
a
23014729
b

TPR Experiments

The TPR results for samples B, C, and D and for $Ni(OH)_2$ are presented in Fig. 3. Samples B, C, and D exhibit an intense peak with a maximum ranging between 500 and 650°C, which slightly shifts with the nickel content. $Ni(OH)_2$, producing a sharp reduction peak around 280°C, is not present in a detectable amount in any sample. The reduction of synthetized Ni-nepouites and Ni-talcs has been studied in the literature (*19, 20*) and a study of the influence of the synthesis conditions on the reducibility of nickel silicates is in progress (*21*). These studies show that Ni-talcs and nepouites synthesized around 150°C present one or two reduction peaks between 500 and 750°C. The TPR profiles obtained with samples B, C, and D are consistent with the presence of silicates in Ni/SiO_2 materials prepared by deposition–precipitation.

Electron Microscopy Study

Electron micrographs of samples C and D are presented in Fig. 4. One can observe platelet structures, which were not present on silica before deposition–precipitation and whose size is larger than 200 Å. The comparison between sample C (7.5 wt% Ni) and sample D (17.5% wt% Ni) illustrates the different extent of reaction of the silica. The platelet structure may be attributed to nickel silicates in accordance with Hermans and Geus (*22*).

X-ray Diffraction

All the samples prepared by deposition–precipitation were found to be X-ray amorphous.

DISCUSSION

The characterization of unreduced Ni/SiO_2 materials prepared by deposition–precipitation shows a very reactive interaction between Ni(II) ions and the oxide leading to silicate formation. This result is consistent with previous work of Geus (*10*) and Burch and Flambard (*15*), who observed an interaction between the support and the metal ions by monitoring the pH of the nickel(II) solution as a function of the deposition–precipitation time. It is also consistent with previous work of Coenen (*13*) and Montes *et al.* (*14*) who attributed the low reducibility and the high stability against sintering of Ni/SiO_2 materials prepared by deposition–precipitation to strong interactions between the metal ions and the support during preparation. Unfortunately, it is not possible to get any direct proof of silicate formation from X-ray diffraction spectroscopy, the precursors being generally X-ray amorphous or, if not, the diffraction patterns of nickel hydroxide and nickel silicates being difficult to distinguish for poorly crystallized compounds. The attribution of the platelet structure observed in Fig. 4 to nickel silicates as distinct from, for instance, nickel hydroxide epitaxially linked to silicate layers is also questionable.

The EXAFS spectroscopy was shown to be well adapted for investigating ion-support interactions (*23*) and allows identification of the nature of the Ni(II)-silica interaction in this work. The presence of significant amounts (>20%) of dispersed Ni(II) ions grafted on silica would lead to a nickel retrodiffusors number inferior to 6 and thus may be excluded even for low nickel contents. On the other hand, the growth of nickel hydroxide over a monolayer of nickel silicates would lead to a significant decrease of the silicon retrodiffusors numbers; in fact, an examination of the fits in Table 3 shows that N_{Si} is higher or equal to 2 for each sample. The precipitation of nickel hydroxide in the porosity of the silica is also excluded from the TPR experiments, the presence of bulk nickel hydroxide being characterized by a sharp reduction profile below 280°C. The EXAFS spectroscopy shows that the deposition–precipitation of Ni(II) on silica from nitrate solutions by the urea method leads to nickel silicate formation independently of the nickel loading. Accepting that XOA 400 silica contains ca 4.6 $\times 10^{18}$ silanol sites per square meter (*16*),

the nickel content involving two silanol sites for each Ni(II) adsorbed ion (*9*) should reach 9 wt%. The obtainment of higher metal loadings shows that silicon ions are extracted from the silica network or, in other words, that the silica partially dissolves during the deposition–precipitation. It is likely that the deposition–precipitation of nickel on silica consists of the growth of silicate layers which are able to attract Ni^{2+} and $Si(OH)_5$-ions from the remaining solution, while a part of the support dissolves. This dissolution is obviously favored by the high specific area of the XOA 400 silica.

The EXAFS spectroscopy allows identification of the nature of the formed silicates. The number of Si next nearest neighbors of the adsorbed Ni(II) ions is found to be independent of the nickel content, its values always close to 2.5, as is the value found for synthesized Ni-nepouites (Table 2). This seems to indicate that the major part of the hydroxysilicates is of nepouite-like structure. The nepouite structure consists of the superimposition of sheets composed of one layer of tetrahedra (SiO_4 units) and one layer of octahedra (NiO_6 units). The presence of a minor part of silicates of talc-like structure, each layer of octahedra (NiO_6 units) being surrounded by two layers of tetrahedra (SiO_4 units), instead of one layer of tetrahedra in the case of the nepouite-like structure, cannot be excluded on the basis of EXAFS experiments. The reduction profiles of synthesized Ni-nepouites and Ni talcs being very dependent on the temperature of synthesis (*21*), the TPR method does not allow us to determine more accurately the amount of talc-like silicates.

A strong interaction with silica during deposition–precipitation has also been observed with Cu(II) (*10*). A TPR and a IR investigation (*24, 25*) showed that this interaction was due to hydroxysilicate formation similar to Ni(II) as reported here. However, another EXAFS study showed that the deposition–precipitation of Cu(II) on silica was possible at low pH (pH 3.5) (*26*). In these samples the number of Si next nearest neighbors was found to be inferior to 1. Thus the silica support only played the role of heterogeneous germ for precipitation with hydroxide $Cu(OH)_2$ or basic copper nitrate $Cu_2(NO_3)(OH)_3$ (*24*) growing around the nuclei. This behavior was never observed in the case of Ni(II) deposition–precipitation.

CONCLUSIONS

The TPR method in conjunction with EXAFS spectroscopy appears to be well adapted to the study of Ni/SiO_2 materials and probably of other systems such as Cu/SiO_2 or Fe/SiO_2. The determination by EXAFS spectroscopy of the composition of the second coordination shell of adsorbed Ni(II) ions evidences the formation of hydroxysilicates of Ni-nepouite-like structure, which are amorphous relatively to X-ray diffraction experiments. TPR analysis does not show any detectable amount of nickel hydroxide retained in the pores of the support after washing.

ACKNOWLEDGMENTS

The authors express their gratitude to C. Marcilly (IFP, Rueil-Malmaison) for his interest and advice on catalyst preparation, A. Decarreau (Université de Poitiers) for the gift of reference samples, F. Villain (LURE, Orsay) for her support during the EXAFS experiments, and E. Copin for the XRD study.

REFERENCES

1. Che, M., and Bonneviot, L., *in* "Successful Design of Catalysts" (T. Inui, Ed.), p. 147. Elsevier, Amsterdam, 1988.
2. Che, M., Clause, O., and Bonneviot, L., *in* "Proceedings, 9th International Congress on Catalysis, Calgary, 1988" (M. J. Phillips and M. Ternan, Eds.), Vol. 4, p. 1750. Chem. Institute of Canada, Ottawa, 1988.
3. Weisz, P. B., *Trans. Faraday Soc.* **63,** 1801 (1967).
4. Weisz, P. B., and Hicks, J. S., *Trans. Faraday Soc.* **63,** 1807 (1967).
5. Clause, O., Bonneviot, L., Che, M., Verdaguer, M., Villain, F., Bazin, D., and Dexpert, H., *J. Chim. Phys.* **86,** 1767 (1989).
6. Bonneviot, L., Clause, O., Che, M., Manceau, A., and Dexpert, H., *Catal. Today* **6,** 39 (1989).
7. Kosawa, A., *J. Inorg. Nucl. Chem.* **21,** 315 (1961).
8. Anderson, J. H., *J. Catal.* **26,** 277 (1972).
9. Bonneviot, L., Legendre, O., Kermarec, M., Oliv-

ier, D., and Che, M., *J. Colloid Interface Sci.* **134,** 534 (1990).

10. Geus, J. W., *in* "Preparation of Catalysts III" (G. Poncelet *et al.*, Eds.), p. 1. Elsevier, Amsterdam, 1985.
11. Bonneviot, L., Clause, O., Che, M., Manceau, A., Decarreau, A., Villain, F., Bazin, D., and Dexpert, H., *Physica B* **158,** 43 (1989).
12. Richardson, J. T., Dubus, R. J., Crump, J. G., Desai, P., Osterwalder, U., and Cale, T. S., *in* "Preparation of Catalysts II," (B. Delmon *et al.*, Eds.), p. 131. Elsevier, Amsterdam, 1979.
13. Coenen, J. W. E., *in* "Preparation of Catalysts II" (B. Delmon *et al.*, Eds.), p. 89. Elsevier, Amsterdam, 1979.
14. Montes, M., Soupart, J. B., De Saedeleer, M., Hodnett, B. M., and Delmon, B., *J. Chem. Soc., Faraday Trans. 1* **80,** 3209 (1984).
15. Burch, R., and Flambard, A. R., *in* "Preparation of Catalysts III" (G. Poncelet *et al.*, Eds.), p. 311. Elsevier, Amsterdam, 1985.
16. Iler, R. K., "The Chemistry of Silica," p. 637. Wiley, New York, 1979.
17. Van Dillen, J. A., Geus, J. W., Hermans, L. A. M., and Van der Mejden, J., *in* "Proceedings, 6th International Congress on Catalysis, London, 1976" (G. C. Bond, P. B. Wells, and F. C. Tompkins, Eds.), p. 677. The Chemical Society, London, 1976.
18. Manceau, A., and Calas, G., *Clay Miner.* **21,** 341 (1986).
19. Martin, G. A., Renouprez, A., Dalmai-Imelik, G., and Imelik, B., *J. Chim. Phys.* **67,** 1149 (1970).
20. Wendt, G., and May, M., *Z. Chem.* **26,** 117 (1986).
21. Clause, O., Kermarec, M., Carriat, J. Y., Decarreau, A. and Che, M., to be published.
22. Hermans, L. A. M., and Geus, J. W., *in* "Preparation of catalysts II" (B. Delmon *et al.*, Eds.), p. 113. Elsevier, Amsterdam, 1979.
23. Clause, O., Bonneviot, L., Che, M., and Dexpert, H., *in* "Proceedings, 2nd European Conference on Progress in X-ray Synchrotron Radiation Research" (A. Balerna, E. Bernieri, and S. Mobilio, Eds.), p. 559. Bologna, 1990.
24. Van der Grift, C. J. G., Elberse, P. A., Mulder, A., and Geus, J. W., *Appl. Catal.* **59,** 275 (1990).
25. Van der Grift, P. A., Mulder, A., and Geus, J. W., *Appl. Catal.* **60,** 181 (1990).
26. Clause, O., Thesis, Université P. et M. Curie, Paris, 1989.